A spatially resolved mechanistic growth law for cancer drug development

Adam Nasim[1], James Yates[2], Gianne Derks[1], and Carina Dunlop[1]

[1]Department of Mathematics, University of Surrey, Guildford, GU2 7XH,UK

[2]Oncology R&D, AstraZeneca, Cambridge,UK

May 3, 2021

Abstract

Mathematical models used in pre-clinical drug discovery tend to be empirical growth laws. Such models are well suited to fitting the data available, mostly longitudinal studies of tumour volume, however, they typically have little connection with the underlying physiological processes. This lack of a mechanistic underpinning restricts their flexibility and inhibits their direct translation across studies including from animal to human. Here we present a mathematical model describing tumour growth for the evaluation of single agent cytotoxic compounds that is based on mechanistic principles. The model can predict spatial distributions of cell subpopulations, tumour growth fraction as well as include spatial drug distribution effects within tumours. Importantly, we demonstrate the model can be reduced to a growth law similar in form to the ones currently implemented in pharmaceutical drug development for pre-clinical trials so that it can integrated into the current workflow. We validate this approach for both

cell-derived xenograft (CDX) and patient-derived xenograft (PDX) data. This shows that our theoretical model fits as well as the best performing and most widely used models. Our work opens up current pre-clinical modelling studies to also incorporating spatially resolved and multi-modal data without significant added complexity and creates the opportunity to improve translation and tumour response predictions.

Significance: A mechanistic model is presented that has the same growth law structure as currently used models for cancer drug development. However, deriving from the mechanistic framework the model is shown to also predict necrotic and growth fractions in the tumour as well as account for variations in spatial drug distribution.

Introduction

Preclinical evaluation of drug efficacy plays a fundamental role in the development of oncological treatments, with the aim being to predict pharmacologically active drug concentrations and guide dose exploration in the clinic. Data for these studies comes from longitudinal measurements of tumour volume in animal models with specific tumours targets being investigated by the use of transplantable tumours with both cell-derived xenograft (CDX) and patient-derived xenografts (PDX) common [1]. Central to these preclinical studies is the use of mathematical equations to describe the tumour dynamics, fit the experimental data, and evaluate the anti-tumour effect. These *mathematical* models usually take the form of simple growth laws for tumour volume with drug action accounted for through an additional loss term. In general they are not spatially resolved. There are many such models which can satisfactorily capture the dynamics when fitted to preclinical data [2, 3, 4, 5, 6, 7], so that for any given data set it is in practice very difficult to distinguish between them [5, 6, 8, 9, 10]. This is compounded by the fact that typically these growth functions are purely empirical descriptions of the data, not founded in a mechanistic description of the physiological process further reducing the ability to discriminate.

Despite the clear successes of pre-clinical modelling there is a key gap in translation to clinical trials. It is acknowledged that a key challenge in pharmaceutical development is that only a very few anticancer drug treatments which are successful pre-clinically, pass through clinical trials and reach the market [11, 12, 13, 14]. This is sometimes known as the attrition rate problem. The reasons for this are complex, but from a mathematical modelling perspective current pre-clinical growth laws cannot be fit-for-purpose in this translational context as they lack the flexibility to account for the significant physiological processes that are being proven to be key [15, 16, 17, 18]. We particularly highlight that the current framework lacks mechanistic underpinnings. For example, it does not account for spatial distributions of key compounds and for tissue structure, meaning that drug distribution and growth fraction cannot be included in the equations despite their increasingly clear significance to treatment response [16, 19]. There has been significant progress in the mathematical modelling of tumour growth in which increasingly sophisticated and mechanistically-founded models have been developed. These modelling approaches span the spectrum from spatial continuum models to large-scale individual-based simulations of cell dynamics [20, 21, 22]. These studies have clearly demonstrated that a range of factors will each have significant implications for in-patient tumour dynamics. Unfortunately, the complexity of these models means that each study tends to focus on one or a few mechanistic aspects with a unified mathematical cancer model still lacking.

The extension of growth law modelling away from purely phenomenological laws into mechanistic modelling would have significant advantages. It would enable better discrimination between models, could improve translational efficacy and be flexible enough to incorporate new multi-modal data sets as they come online. However, from a practical perspective, more complex, mechanistically founded mathematical models and simulations raise significant additional challenges in use in pre-clinical studies. In general they have many more parameters than the current growth laws used, which makes it challenging to parameterise them given the typical data collected in CDX and PDX studies. Specifically

this causes significant difficulty with parameter identifiability, with model over-parameterisation a key issue. Indeed, access to suitable data is acknowledged as significant issue for applications of mechanistic models [4]. This challenge is being met by the implementation of additional imaging modalities including MRI [23], generating multi-modal data sets. However, robust methods for integrating these data types into pre-clinical trials are still under development.

It has been challenging to quantitatively translate the efficacy seen in animal models and this lack of translation has been suggested as the root cause for the high rate of failure [13]. However, it has been shown that drug exposure-response relationships can be translated [24] and that taking this into account can contribute to an improved success rate [25]. One aspect that is clearly different between animal models of cancer and patients' tumours is the rate of growth and this will impact response to therapy [26]. It is hypothesised that accounting for these differences mechanistically, translation will be improved further. Here, we present a mechanistic mathematical model for tumour growth that takes the form of a simple growth law but which incorporates growth limitation through nutrient availability. This model is based on a well-accepted mathematical framework for spatial models of tumours which couples spatial diffusive processes to tumour growth [27]. Significantly, its mechanistic foundations ensure that it can predict the size of the growing fraction of the tumour over time. This is obtained by determining from the spatial model the regions of the tumour that are sufficiently oxygenated or nutrient rich for proliferation. Importantly, by making simplifying assumptions about tumour geometry we show that this model can be expressed as a growth law of a similar type to that currently used in the pharmaceutical industry. It thus can be fitted and analysed using current industry-standard methods. We demonstrate the ease of use by comparison with a current commonly adopted growth law [2] and validate both the models using standard methods on CDX and PDX data. The model also shows how tracking the predicted growth fraction will alter treatment dynamics, validated by end point histology. We also demonstrate that the new framework offers additional significant advantages such as being able to account

Model	K_V	Parameters
Linear	$\frac{a}{V}$	2
Exponential	a	2
Logistic	$a - bV$	3
Gompertz	$a - b\ln(V)$	3
Exponential-linear [2]	$\frac{a_0}{\left[1+\left(\frac{a_0}{a_1}V\right)^{\psi}\right]^{\frac{1}{\psi}}}$	4*
Surface growth [28]	$aV^{-\frac{1}{3}}$	2
Proliferative rim [29]	$a\left(1-\left(1-\frac{r_d}{(\frac{3V}{4\pi})^{\frac{1}{3}}}\right)^3\right)$	3

Table 1: Common growth models used for pre-clinical modelling. The parameter a is the growth rate and b the rate of natural death. In the exponential-linear model a_0 and a_1 are the growth rates in the exponential and linear phases, respectively with ψ describing the transition between these phases. The number of model fit parameters for each model includes the initial tumour volume. (*: ψ is typically taken as 20, for a smooth and fast transition between phases, in this case it effectively becomes a three parameter system.)

for spatial gradients in drug distribution without requiring significantly more complex models. Together we see our model is fit-for-purpose to bridge the gap between emerging multi-modal data availability and the current pre-clinical trial workflow.

Materials and Methods

Mathematical growth laws for tumour growth and treatment effect

Mathematical models as used in pre-clinical studies typically take the form of empirically derived growth laws for tumour volume. These models are ideally suited to the longitudinal data typically available from animal model studies.

Mathematically these models can be expressed as a rate change equation for the tumour volume $V(t)$ of the form

$$\frac{dV}{dt} = K_V(V)V - L_{\text{Drug}}(w)V, \tag{1}$$

with a condition on the initial tumour volume that $V(t = 0) = V_0$, which is usually taken as a fit parameter of the system. The function $L_{\text{Drug}}(w)$ describes cell loss as a function of the drug concentration $w(t)$. Simple functional forms are typically assumed for $L_{\text{Drug}}(w)$, most often it is taken as linear so that $L_{\text{Drug}}(w) = K_{\text{kill}}w$. The function $K_V(V)$ represents the net growth rate of the tumour, with a range of different forms used in pre-clinical studies [4, 6, 14] (Table 1) with the form often chosen to optimise data fitting. For example, where the growth is observed to be linear $K_V(V) = a/V$, whereas exponential growth is captured by K_V being constant.

Although all the models from Table 1 have successfully been used to fit pre-clinical data there are some significant structural differences. The first five (linear, exponential, logistic, Gompertz, and exponential-linear) can be considered as empirical growth laws with model parameters that are hard to link directly to meaningful biological parameters. The other two models, however, attempt to e.g. also allow for the experimental observation that only cells nearer the edge of the tumour proliferate. Mayneord [28] thus assumes surface growth only, while the model of Evans et al. [29] alternatively assumes proliferation in a rim of fixed thickness. One drawback of all these growth models, except the Gompertz and logistic models, is that they predict unbounded growth as time increases. In contrast, the Gompertz and logistic models exhibit growth retardation before reaching a stable, constant tumour volume. Despite these manifest differences in dynamics all the listed models can adequately describe the animal-derived data, as the data cannot be obtained over long enough timescales for any growth retardation to be clearly observed. However, how this impacts on clinical studies is less clear where the observation timescales are longer although there are still natural limits to data collection.

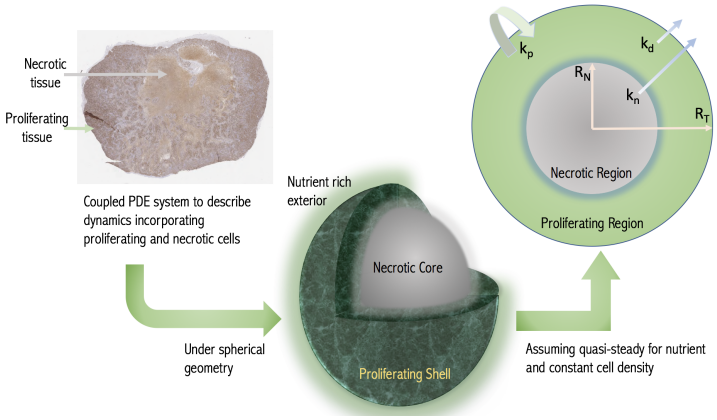

Figure 1: Schematic of the modelling concept. A growing tumour is modelled as a proliferating shell encapsulating a necrotic (non-proliferative core) with the boundaries between regions determined dynamically by considering nutrient diffusion. The assumed geometry and model variables and parameters are labelled in the cross-section with R_N and R_T being the necrotic and total tumour radii respectively. (Histological image a day 24 CDX xenograft with Ki-67 stain.

Diffusion-limited mechanistic model for tumour growth and treatment effect

An alternative approach to modelling tumour growth, that has been popular in the modelling literature, has been to model directly the spatial diffusion of nutrients within tumours directly. It is assumed that nutrient availability determines the status of the cell, with cells experiencing sufficiently low nutrient levels undergoing necrosis. This results in a map of the tumour with different sized cellular compartments for e.g. proliferative and non-proliferative necrotic compartments determined responsively from the environmental conditions [27, 30], see Fig. 1. This basic framework has been extensively built upon in the mathematical literature to model a range of different effects and scenarios, see reviews [20, 31]. These increasingly complex models are typically expressed in terms of partial differential equations which are either solved numerically themselves or coupled into finer scaled simulations.

We adopt this mechanistic diffusion-based framework but make simplifying assumptions which are realistic in the pre-clinical context and reduce the partial differential equations to a growth law of the form Equation (1), for the full details see the Supplementary Information. The method is based on assuming a spherical tumour with the depth of penetration of nutrient within the tumour determined from the diffusion equation. From this solution we obtain the growth fraction (GF) of the tumour, i.e. the volume fraction of tumour that is proliferating ($GF = 1$ represents fully proliferating). A key parameter is the volume V^* at which the tumour first experiences necrosis. This enables the tumour volume to be determined from a conservation of mass argument as the regions in which cells are lost or gained are now mechanistically determined. The resulting model is similar to Equation (1), but with the growth fraction accounted for i.e.

$$\frac{dV}{dt} = K_V(V)V - L_{\text{Drug}}(w, GF)V, \tag{2}$$

$$K_V = (k_p - k_d)GF - k_n(1 - GF), \tag{3}$$

$$V^* = V(1 + 2(1 - GF)^{\frac{1}{3}})^{\frac{3}{2}}(1 - (1 - GF)^{\frac{1}{3}})^3, \quad V > V^*, \tag{4}$$

and $GF = 1$ when $V < V^*$. The initial condition is $V(0) = V_0$. In this model, k_p is the constant rate at which cells in the proliferating region replicate, k_d is the constant rate at which cells die and get removed from the proliferating region and k_n is the constant rate of breakdown and removal of tissue within the necrotic region. Key is that while the volume of the tumour $V < V^*$, the entire volume of tumour proliferates and the model predicts exponential growth before switching to diffusion limited growth as the volume increases with the growth fraction then determined from Equation (4).

The formulation Equations (2) to (4), which we term the diffusion-limited model, facilitates simple numerical solution and can be incorporated easily into pre-clinical data fitting protocols being of the same mathematical form as currently implemented. However, it is now possible to directly predict the proliferating compartment and growth fraction of the tumour. We will demonstrate the

functionality of the description Equations (2) to (4) both for control data sets and for drug trial data. To account for the drug action we take unless otherwise stated that $L_{\mathrm{Drug}}(w, GF) = K_{\mathrm{kill}}\, GF\, w$. This is superficially similar to the standard cell loss term, however cell loss now only occurs in the proliferating compartment determined by GF, see the Supplementary Information for full details. Already, we see that a mechanistic approach allows the model to incorporate a key feature of most cell cycle specific pharmaceutical agents that they will target only proliferating cells. The pharmacokinetic (PK) description is in general compound specific. Here we consider the compound CPT-11 (Irinotecan) which has been shown to be adequately described by an exponential PK model [18], thus $w = w_0 \exp(-\alpha t)$, with w_0 the administered dose and α the rate of natural decay. With the half life of Irinotecan being 12 hours, this gives $\alpha = 1.39\,\mathrm{day}^{-1}$, which we take throughout.

Numerical implementation

The system Equations (2) to (4) takes the form of a growth law and two constraints and can be numerically solved as an algebraic differential equation (ADE). However, given current fitting protocols based on nonlinear mixed effects fitting (NLME) it is easier to work with a system of differential equations. This may be obtained from Equations (2) to (4) by differentiating the constraint Equation (4). The routines are implemented within MATLAB2019a (MathWorks, Natick, MA). Due to the significant inter-subject heterogeneity we use a nonlinear mixed effects fitting approach (NLME) to fit both the population and individual subject parameters using the stochastic approximation expectation-maximization algorithm (SAEM) as implemented in MATLAB. Within the SAEM algorithm the probit transform is implemented to ensure all parameters remain positive. See Supplementary Information for full details.

Data sets used for model validation

Control data are from AstraZeneca mouse-derived cell line xenografts (CDXs) for two different cell-lines SW620 (29 mice), epithelial colorectal adenocarcinoma, and Calu6 (178 mice), epithelial lung adenocarcinoma. With regards treatment data we consider SW620 CDXs (95 mice) which were treated with weekly doses of 50mg/kg of CPT-11 (Irinotecan) either three times on days 1,8,15 which we label protocol 1, (68 mice), or four times during the experiment on days 1,8,15,22 (protocol 2, 18 mice) or 4,11,18,25 (protocol 3, 9 mice).

Additionally, we use the Novartis patient-derived xenograft (PDX) dataset, which is the largest publicly available database of PDX control data [32]. The Novartis data contains 226 mice with six different tumour types, namely breast carcinoma (BRCA) 39 mice, non-small cell lung carcinoma (NSCLC) 28 mice, gastric cancer (GC) 44 mice, colorectal cancer (CRC) 45 mice, cutaneous melanoma (CM) 33 mice, and pancreatic ductal carcinoma (PDAC) with 37 mice.

All animal studies in the United Kingdom were conducted in accordance with the UK Home Office legislation, the Animal Scientific Procedures Act 1986, and with AstraZeneca Global Bioethics Policy.

Results

Demonstration of the functionality of the model in fitting pre-clinical data

To demonstrate the ability of the diffusion-limited growth model to fit to longitudinal pre-clinical CDX growth data we consider the AstraZeneca CDX data, see Methods. In Fig. 2A–D we show the individual fits of the diffusion-limited model to the experimental data both combined and separated into the individual protocols. The diffusion-limited model is observed to fit well by eye across the range of growth curves and treatment protocols. Similarly qualitatively good fits are observed for the other CDX and PDX control data sets (Fig. S.1). To further demonstrate visually the quality of fit we perform a visual predic-

tive check (VPC) analysis [33]. This confirms that the diffusion-limited model captures the full range of dynamics of the CDX data (Fig. 2E and F). Similar results are also obtained from visual predictive checks for the other control PDX and CDX data sets (Fig. S.2).

Although the visual checks indicate a good quality of fit we need to also quantify how well the model performs. Looking at the NLME results for the fit of the diffusion-limited model for the CDX data in Table 2 we see a small residual mean square error (rsme) indicating a good quality of fit. We further compare the fit to results obtained from one of the most widely used models, the exponential-linear model [2], which is often used as a reference model [18, 34]. The NLME parameter estimation for the treated animals for both the exponential-linear and diffusion-limited models is given in Table 2. We also show in Fig. 2G five representative fits for this data with the simulated curves generated by their individual parameter estimates. We clearly see the similarity in the model behaviour. This similarity in the quality of fit to the data between the two models is further confirmed by the closeness of the Akaike information criterion number (-217 and -221, for the diffusion-limited and exponential-linear respectively) and root mean square error (0.146 and 0.142, respectively) (Table 2). A similar result is achieved when considering the control data sets. These results are summarised in the supplementary information Tables S.1 to S.8. Given the typically limited time course of pre-clinical data it has been shown across numerous studies no model may be optimal across all data sets [4, 6, 10], however, the results indicate that the diffusion-limited model provides a similar standard of fit as current models for typical data.

Diffusion-limited model predicts growth fraction dynamics with tumours

As discussed and shown in the Supplementary Information, the governing equations are obtained by solving and reducing a coupled system including a spatial model for nutrient diffusion. As such, the rate equation thus derived automati-

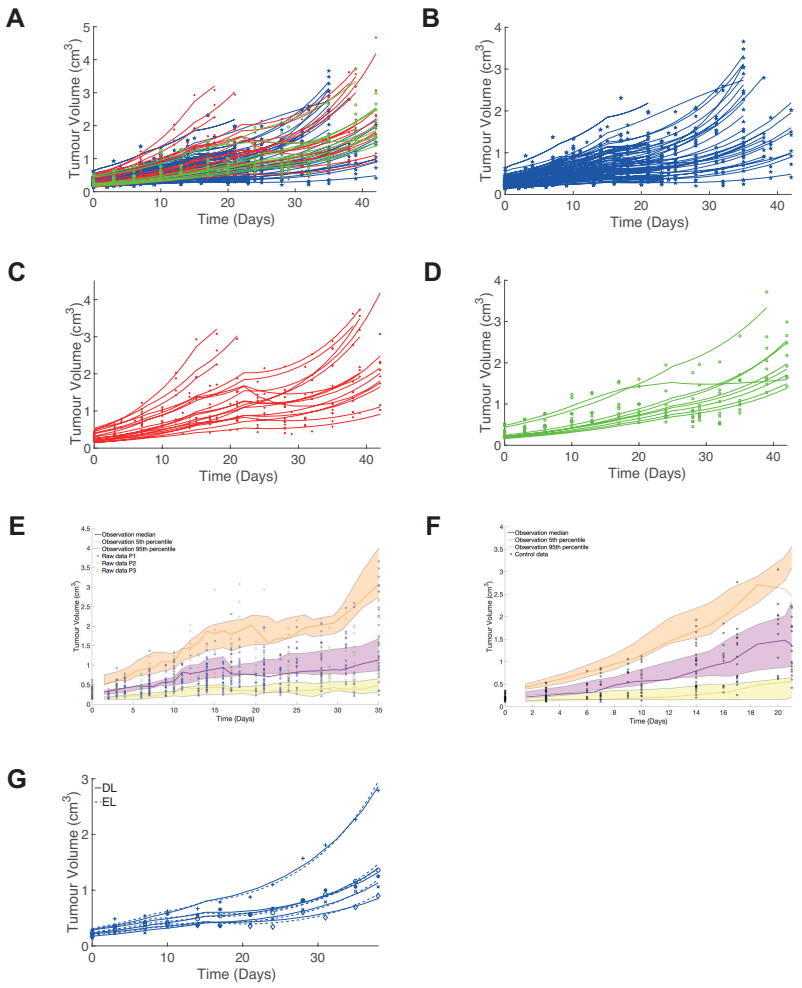

Figure 2: **A**, Fit of the diffusion-limited model to all CDX treatment data colour coded by treatment protocol (95 subjects, SW620 cell line, see Methods). **B**–**D** Fits separated by treatment protocol for clarity. **E** and **F**, Visual predictive checks (VPC) of both the treated and control CDX data. The VPC is based on 1000 simulations, the shaded regions represent the 95% confidence intervals (CI) of the 25th, 50th and 95th percentiles of the simulated data. The experimental data median, 25th and 95th percentiles are marked (obtained using rolling average). **G**, Fit of both the diffusion-limited and exponential-linear models to five representative data sets from protocol 1.

Model	Parameter	Definition	Value	SD	rmse	AIC
DL	$k_p - k_d$	Net growth rate(day^{-1})	0.12	0.02	0.146	-217
	k_n	Necrotic loss rate(day^{-1})	0.05	0.03		
	K_{kill}	Drug potency(ng^{-1}ml day^{-1})	5.7×10^{-3}	2.4×10^{-4}		
	$R^*(= (3V^*/4\pi)^{1/3})$	Critical Radius(cm)	0.41	0.07		
	V_0	Initial Volume(cm^3)	0.25	0.11		
EL	λ_0	Exponential growth rate(day^{-1})	0.08	0.25	0.142	-221
	λ_1	Linear growth rate(day^{-1})	0.31	0.06		
	$\hat{k}(= k_1/30)$	Transient death rate (day^{-1})	24	6.2		
	K_{kill}	Drug potency (ng^{-1}ml day^{-1})	1.2×10^{-3}	4×10^{-4}		
	V_0	Initial Volume(cm^3)	0.29	0.13		

Table 2: NLME results of 10 runs for the full AstraZeneca CDX data set of 95 mice, see Methods, for the diffusion-limited (DL) and exponential-linear (EL) models.

cally tracks dynamically the growth fraction of the tumour, GF, through Equation (4). Thus in addition to being able to fit the model to longitudinal measurements of tumour size we can predict how the corresponding growth fraction changes including in response to treatment. We show, for example, in Fig. 3A that those tumours showing greatest response to treatment (at dosing strengths 75 and 100 mg/kg) are predicted to also experienced the largest increase in growth fraction with consequent implications for treatment success.

The growth fraction of tumours during drug trials is normally unavailable due to the difficulties of accessing this information *in vivo*. However, at the termination of xenograft experiments it is possible to access growth fraction data through histology although this is not routinely done. We consider independent data sets for the necrotic area for untreated SW620 and Calu6 cell lines obtained from histology of selected bisected tumours (Ki-67 staining). This histological staining labels the proliferating cells in a cross-section of the tumour and from this the necrotic *area*, N_{area}, may be determined. The total growth fraction GF and necrotic area are related by $N_{\text{area}} = (1 - GF)^{\frac{2}{3}}$ for a spherical tumour. We simulate tumour dynamics for a control tumour using the population parameters obtained from the mixed effects fitting of CDX data Tables S.1 and S.2. We see that these simulations predict a necrotic area at the end of the experiment for both the SW620 cell line and the Calu6 cell lines that fits the experimental data

(lying within the range of the data in Figs. 3B and C). Note in this case, we use the necrotic area data as an independent dataset. We could have instead used this data to further calibrate the model parameters. This highlights one of the benefits of a mechanistic model formulation, that we can utilise other sources of information to better calibrate the model by way of multimodal fitting.

Incorporation of spatial gradients in drug concentrations

Finally, we demonstrate the flexibility of the mechanistic modelling framework by demonstrating how not only spatial gradients of nutrients but also drug distribution can be captured and easily incorporated in the model. This extended model, while more complex, is equally straightforward to numerically implement requiring a single additional integration. For the mathematical details see the Supplementary Information. The central concept is that, just as for nutrient distribution, the spatial distribution of the drug can be determined from a diffusion equation. Under certain assumptions, primarily the standard and justifiable assumption that diffusion is a fast process compared with cell growth, this allows the spatial solution for drug distribution to be simply coupled into the ODE system.

As a specific example, we consider the case that the action of the drug is considered to be that cell loss occurs in proliferating cells only with the drug kill linearly dependent on drug concentration as before. However, now the drug distribution is not constant throughout the tumour. In this case, the cell loss term is

$$L_{\mathrm{Drug}}(w, GF) = 3 \int_{(1-GF)^{\frac{1}{3}}}^{1} s^2 K_{\mathrm{Kill}} w(t, R_T s) ds \tag{5}$$

where R_T is the tumour radius, with for a spherical tumour $R_T = (3V/4\pi)^{1/3}$.

When the drug concentration is constant throughout the tumour we recover $L_{\mathrm{Drug}} = K_{Kill}\, GF\, w$ from the integral. For a drug diffusing into the tumour, however, drug distribution is not constant and in this case the model predicts

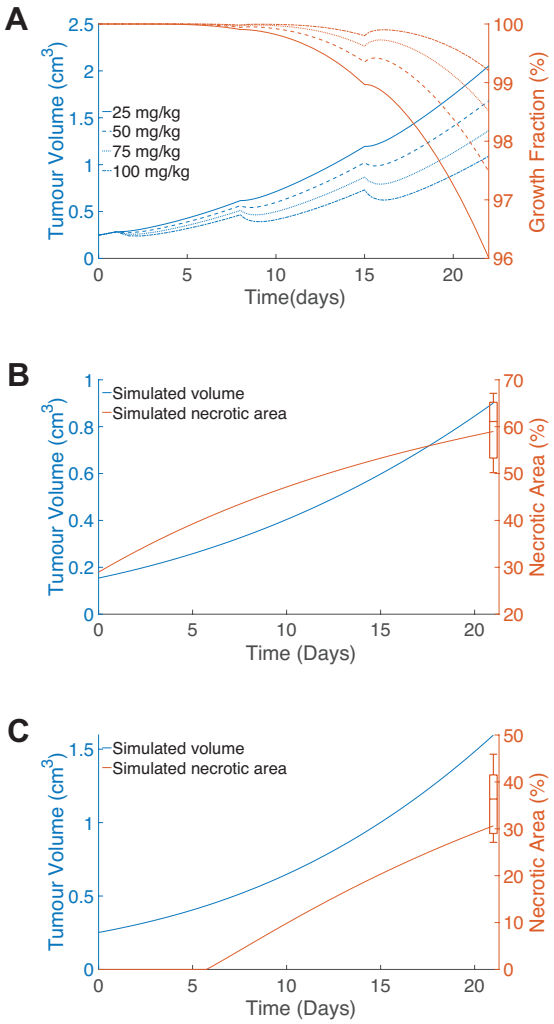

Figure 3: **A**, Simulated tumour response along with the predicted growth fraction for dosing strengths 25,50,75 and 100mg/kg dosed on days 1,8,15. **B**, and **C**, Simulated tumour dynamics for the CDX xenografts (**B**, SW620 and **C**, Calu6 cell lines, simulated curves using population parameters from Tables S.1 and S.2. The end-point box plots are derived from histological examination of necrotic area for 8 SW620 xenografts and 10 Calu6 xenografts.

the drug concentration distribution (see Supplementary Information) as

$$w(t,r) = \frac{w_{\text{ext}}(t)(I_0(Fr) + MK_0(Fr))}{I_0(FR_T) + MK_0(FR_T)}, \tag{6}$$

where $w_{\text{ext}}(t)$ is the time varying applied drug concentration, I_0 and K_0 are the modified Bessel functions of zero order. The constant M is a known parameter defined in terms of the other model parameters (see Supplementary Information). Although more complex than the previous model with w spatially constant, this solution is easily implemented into most numerical solvers as it is an explicit solution in terms of the standard built-in functions (I_0 and K_0) and requires a single numerical integration step.

The new drug model introduces the key additional parameter $F = \sqrt{\frac{lh+K_{\text{kill}}}{hD_w}}$, where l is the natural decay rate of the drug, h the efficiency of the drug and D_w the drug diffusivity. The parameter F effectively quantifies the depth of penetration of the drug into the tissue with $F = 0$ corresponding to full drug distribution throughout the tumour and F large corresponding to a surface kill effect. F is, however, not anticipated as a free fit parameter given that the drug penetration is usually known. Heatmaps showing drug concentration within the tumour clearly demonstrate a strong effect of F on the amount of drug penetrating into the tumour (Fig. 4A). As F increases the amount of drug that can penetrate fully into the tumour drops significantly, indeed by the time $F = 5$ the concentration drops to 27% percent of its concentration at the outside edge (Fig. 4B). Exploring the effect on the tumour dynamics of modelling the spatial distribution of the drug, we plot a representative solution of the spatially dependent drug model (Fig. 4C). We see that as the drug penetration is reduced (F increased), the tumour displays a more linear-like growth. With greater drug penetration (F small), a greater effect is observed with faster dynamic rebounds. Overall, it is clear tumour response varies depending on the drug distribution when the drug potency and dose strength remains fixed.

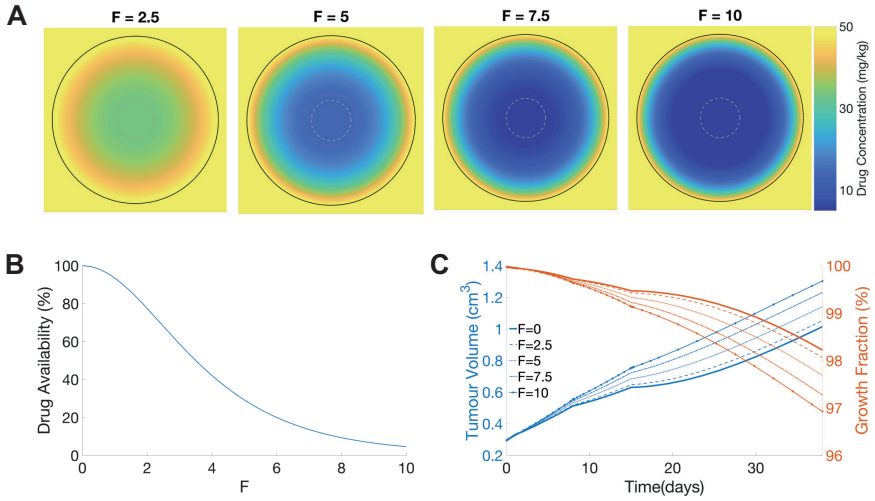

Figure 4: **A**, Heat map of the simulated internal drug distribution within the tumour immediately following dosing on day 15. The grey dashed circle shows the predicted necrotic region. The tumour edge is indicated by the black solid line. **B**, Percentage of drug concentration reaching inner necrotic radius (corresponding to grey circle in **A**) as a function of drug localization parameter F. **C**, Tumour volume and growth fraction dynamics for dosing strength fixed at 50mg/kg dosed on days 1,8,15. $F = 0$ describe full drug distribution, with F increasing corresponding to reducing drug penetration. At $F = 10$ the drug effect is largely restricted to the surface of the tumour.

Discussion and Conclusions

We have presented here a mathematical model for tumour growth and treatment that is based on a mechanistic description of nutrient limited growth. Despite being derived from spatial partial differential equations we show that these equations can be reduced to a growth law which is not significantly more complex than those currently used for pre-clinical drug trials. This simplification is based on assuming a spherical geometry and exploiting the difference in timescales of growth and diffusion to decouple the two partial differential equation systems.

The development of a mechanistic approach has several advantages over more phenomenological growth laws. Perhaps most significantly, in its current form the model allows for the dynamic prediction of the growing fraction of the tumour accounting for cell loss in the centre of the tumour from e.g. hypoxia. As most cytotoxic agents target only actively proliferating cells, tracking the growth fraction has potentially significant implications for treatment dynamics. This is only enhanced by the increasingly clear role hypoxia has in inducing downstream biological processes which directly promote tumour resistance to treatment [19, 35, 36, 37, 38]. Although longitudinal growth fraction data is not usually available for xenograft experiments there is increasing interest in using non-invasive methods, such as MRI, to track levels of hypoxia throughout the course of experiments [39, 40]. The increasing incorporation of MRI and other new types of data collection into pre-clinical modelling will only further increase the need for mechanistic models capable of simulating multi-modal data sets easily.

By considering a range of different data sets including PDX and CDX data we have shown that the diffusion-limited model fits the data comparably to current industry standard models. The model fitting was performed using a standard nonlinear mixed effects workflow demonstrating that the growth model derived can be solved comparably to models currently employed. For independent datasets containing growth fraction data at termination we demonstrate that we predict a growth fraction commensurate with that observed. This while

not presenting significant increased complexity in its numerical solution. In addition, the diffusion-limited growth model parameters are all based on observable phenomena: net proliferation rate, maximum volume before necrosis begins, initial volume and cell loss through necrosis. This is in contrast to standard phenomenological models which perform well when being fitted to data as shown in many works [4, 6, 9] but its parameters are often difficult to interpret. The introduction of spatial modelling into a growth law framework has also enabled us to additionally describe how the distribution of drug varies across the tumour. The indicative results obtained demonstrate the potential importance of accounting for this into pre-clinical studies. Indeed, the increasing importance of monoclonal antibody treatments (mAbs), with their reduced diffusivity, and antibody-drug conjugates (ADCs) [41] will only increase the importance of spatial modelling in pre-clinical trials.

The flexibility of mechanistic approaches to tumour modelling is thus seen to enable the incorporation of multi-modal data types as they are collected. We also demonstrate how spatial variations in both nutrient and drug distribution can be included within a growth law framework. Such new modelling information can be expected to increase the accuracy with which drug treatment dynamics can be modelled and inform better decision making in pre-clinical modelling. Mechanistic models based on cellular behaviour should also aid in bridging the translation gap from pre-clinical to clinical trials given the transparency of the model and capability for parameter adjustment across model systems.

Acknowledgements

A. Nasim is grateful for funding provided by the University of Surrey's Doctoral College Grant and additional funding from AstraZeneca. All authors would like to thank AstraZeneca for the generous access to its data and the EPSRC funded QSP-UK network (EP/N005481/1) for facilitating the initial discussions about this research.

References

[1] J.W.T Yates, H. Byrne, S.C. Chapman, T. Chen, J Delgado-SanMartin, G.D. Veroli, S. J. Dovedi, C. Dunlop, R. Jena, D. Jodrell, E. Martin, F. Mercier, A. Ramos-Montoya, H. Struemper, and P. Vicini. Opportunities for quantitative translational modeling in oncology. *Clin. Pharmacol. Ther.*, 108(3):447–457, 2020.

[2] M. Simeoni, P. Magni, C. Cammia, G. De Nicolao, V. Croci, E. Pesenti, M. Germani, I. Poggesi, and M. Rocchetti. Predictive pharmacokinetic-pharmacodynamic modeling of tumor growth kinetics in xenograft models after administration of anticancer agents. *Cancer Res.*, 64(3):1094–1101, 2004.

[3] Benjamin Gompertz. Xxiv. on the nature of the function expressive of the law of human mortality, and on a new mode of determining the value of life contingencies. *Philos. Trans. R. Soc.*, 115:513–583, 1825.

[4] B Ribba, NH Holford, P Magni, I Trocóniz, I Gueorguieva, P Girard, C Sarr, M Elishmereni, C Kloft, and LE Friberg. A review of mixed-effects models of tumor growth and effects of anticancer drug treatment used in population analysis. *CPT Pharmacometrics Syst.*, 3(5):113, 2014.

[5] H. Murphy, H. Jaafari, and H. Dobrovolny. Differences in predictions of ode models of tumor growth: A cautionary example. *BMC cancer*, 16:163, 2016.

[6] S. Benzekry, C. Lamont, A. Beheshti, A. Tracz, J. M. Ebos, L. Hlatky, and P. Hahnfeldt. Classical mathematical models for description and prediction of experimental tumor growth. *PLoS Comput. Biol.*, 10(8):e1003800, 2014.

[7] E. Tjörve and K. M. Tjörve. A unified approach to the Richards-model family for use in growth analyses: why we need only two model forms. *J. Theor. Biol.*, 267(3):417–425, 2010.

[8] M. Kühleitner, N. Brunner, W. G. Nowak, K. Renner-Martin, and K. Scheicher. Best fitting tumor growth models of the von Bertalanffy-PütterType. *BMC Cancer*, 19(1):683, 2019.

[9] D. Voulgarelis and J. Yates. NLME comparison of tumour growth models. *Preprint.*, 2021.

[10] M. Marušić, Ž. Bajzer, S. Vuk-Pavlović, and J.P. Freyer. Tumor growth *in vivo* and as multicellular spheroids compared by mathematical models. *Bull. Math. Biol.*, 56(4):617–631, 1994. PMID: 15209404.

[11] L. Hutchinson and R. Kirk. High drug attrition rates–where are we going wrong? *Nat. Rev. Clin. Oncol.*, 8(4):189–190, 2011.

[12] I. Kola and J. Landis. Can the pharmaceutical industry reduce attrition rates? *Nat. Rev. Drug Discov.*, 3(8):711–715, 2004.

[13] I.W. Mak, N. Evaniew, and M. Chert. Lost in translation: animal models and clinical trials in cancer treatment. *Am. J. Trans. Res.*, 6(2):114–118, 2014.

[14] L. Carrara, S. M. Lavezzi, E. Borella, G. De Nicolao, P. Magni, and I. Poggesi. Current mathematical models for cancer drug discovery. *Expert Opin. Drug Discov.*, 12(8):785–799, 2017.

[15] X. Jing, F. Yang, C. Shao, K. Wei, M. Xie, H. Shen, and Y. Shu. Role of hypoxia in cancer therapy by regulating the tumor microenvironment. *Mol Cancer*, 18(1):157, 2019.

[16] M. A. Aleskandarany, A. R. Green, E. A. Rakha, R. A. Mohammed, S. E. Elsheikh, D. G. Powe, E. C. Paish, R. D. Macmillan, S. Chan, S. I. Ahmed, and I. O. Ellis. Growth fraction as a predictor of response to chemotherapy in node-negative breast cancer. *Int J Cancer*, 126(7):1761–1769, 2010.

[17] P. Gerlee. The model muddle: in search of tumor growth laws. *Cancer Res.*, 73(8):2407–2411, 2013.

[18] S. Wilson, M. Tod, A. Ouerdani, A. Emde, Y. Yarden, A. Adda Berkane, S. Kassour, M. X. Wei, G. Freyer, B. You, E. Grenier, and B. Ribba. Modeling and predicting optimal treatment scheduling between the antiangiogenic drug sunitinib and irinotecan in preclinical settings. *CPT Pharmacometrics Syst. Pharmacol.*, 4(12):720–727, 2015.

[19] S. Riffle and R. S. Hegde. Modeling tumor cell adaptations to hypoxia in multicellular tumor spheroids. *J. Exp. Clin. Cancer Res.*, 36(1):102, 2017.

[20] J. S. Lowengrub, H. B. Frieboes, F. Jin, Y. L. Chuang, X. Li, P. Macklin, S. M. Wise, and V. Cristini. Nonlinear modelling of cancer: bridging the gap between cells and tumours. *Nonlinearity*, 23(1):R1–R9, 2010.

[21] I. M. Chamseddine and K. A. Rejniak. Hybrid modeling frameworks of tumor development and treatment. *Wiley Interdiscip. Rev. Syst. Biol. Med.*, 12(1):e1461, 2020.

[22] J. Metzcar, Y. Wang, R. Heiland, and P. Macklin. A review of cell-based computational modeling in cancer biology. *JCO Clin. Cancer Inform.*, 3:1–13, 2019.

[23] J. C. Walsh, A. Lebedev, E. Aten, K. Madsen, L. Marciano, and H. C. Kolb. The clinical importance of assessing tumor hypoxia: relationship of tumor hypoxia to prognosis and therapeutic opportunities. *Antioxid Redox Signal*, 21(10):1516–1554, 2014.

[24] H. Wong, E.F. Choo, B. Alicke, X. Ding, H. La, E. McNamara, F-P. Thiel, J. Tibbitts, L.S. Friedman, and S.E. Hop, C.E.C.A. Gould. Antitumor activity of targeted and cytotoxic agents in murine subcutaneous tumor models correlates with clinical response. *Clin. Cancer Res.*, 18(14):3846–3855, 2019.

[25] P. Morgan, D.G. Brown, S. Lennard, M. Anderton, J.C. Barrett, U. Eriksson, M. Fidock, B. Hamrén, A. Johnson, R.E. March, J. Matcham, J. Mettetal, D.J. Nicholls, S. Platz, S. Rees, M. Snowden, and M.N. Pangalos. Impact

of a five-dimensional framework on R & D productivity at AstraZeneca. *Nat. Rev. Drug Discovery*, 17:167–181, 2018.

[26] I.F. Tannock. The five Rs of chemotherapy. *Lancet Oncol.*, 17(6):703–705, 2016.

[27] H. M. Byrne and M. A. Chaplin. Growth of necrotic tumors in the presence and absence of inhibitors. *Math. Biosci.*, 135(2):187–216, 1996.

[28] W. V. Mayneord. On a law of growth of Jensen's rat sarcoma. *Clin. Cancer Res.*, 16(4):841–846, 1932.

[29] N. D. Evans, R. J. Dimelow, and J. W. Yates. Modelling of tumour growth and cytotoxic effect of docetaxel in xenografts. *Comput. Methods Programs Biomed.*, 114(3):3–13, 2014.

[30] N.F. Britton. *Essential Mathematical Biology*. Springer, 2005.

[31] H. M. Byrne. Dissecting cancer through mathematics: from the cell to the animal model. *Nat. Rev. Cancer*, 10(3):221–230, 2010.

[32] H. Gao, J. M. Korn, S. Ferretti, J. E. Monahan, Y. Wang, M. Singh, C. Zhang, C. Schnell, G. Yang, Y. Zhang, O. A. Balbin, S. Barbe, H. Cai, F. Casey, S. Chatterjee, D. Y. Chiang, S. Chuai, S. M. Cogan, S. D. Collins, E. Dammassa, N. Ebel, M. Embry, J. Green, A. Kauffmann, C. Kowal, R. J. Leary, J. Lehar, Y. Liang, A. Loo, E. Lorenzana, E. Robert McDonald, M. E. McLaughlin, J. Merkin, R. Meyer, T. L. Naylor, M. Patawaran, A. Reddy, C. Röelli, D. A. Ruddy, F. Salangsang, F. Santacroce, A. P. Singh, Y. Tang, W. Tinetto, S. Tobler, R. Velazquez, K. Venkatesan, F. Von Arx, H. Q. Wang, Z. Wang, M. Wiesmann, D. Wyss, F. Xu, H. Bitter, P. Atadja, E. Lees, F. Hofmann, E. Li, N. Keen, R. Cozens, M. R. Jensen, N. K. Pryer, J. A. Williams, and W. R. Sellers. High-throughput screening using patient-derived tumor xenografts to predict clinical trial drug response. *Nat. Med.*, 21(11):1318–1325, 2015.

[33] M. Bergstrand, A. C. Hooker, J. E. Wallin, and M. O. Karlsson. Prediction-corrected visual predictive checks for diagnosing nonlinear mixed-effects models. *AAPS J*, 13(2):143–151, 2011.

[34] N. Terranova and P. Magni. TGI-Simulator: a visual tool to support the preclinical phase of the drug discovery process by assessing in silico the effect of an anticancer drug. *Computat Methods Programs Biomed*, 105(2):162–174, 2012.

[35] J. M. Brown and W. R. Wilson. Exploiting tumour hypoxia in cancer treatment. *Nat. Rev. Cancer*, 4(6):437–447, 2004.

[36] S. Strese, M. Fryknäs, R. Larsson, and J. Gullbo. Effects of hypoxia on human cancer cell line chemosensitivity. *BMC Cancer*, 13:331, 2013.

[37] L. Zheng, C. J. Kelly, and S. P. Colgan. Physiologic hypoxia and oxygen homeostasis in the healthy intestine. A review in the theme: Cellular responses to hypoxia. *Am. J. Physiol. Cell Physiol.*, 309(6):C350–360, 2015.

[38] S. Daster, N. Amatruda, D. Calabrese, R. Ivanek, E. Turrini, R. A. Droeser, P. Zajac, C. Fimognari, G. C. Spagnoli, G. Iezzi, V. Mele, and M. G. Muraro. Induction of hypoxia and necrosis in multicellular tumor spheroids is associated with resistance to chemotherapy treatment. *Oncotarget*, 8(1):1725–1736, 2017.

[39] D. A. Hormuth, J. A. Weis, S. L. Barnes, M. I. Miga, E. C. Rericha, V. Quaranta, and T. E. Yankeelov. A mechanically coupled reaction-diffusion model that incorporates intra-tumoural heterogeneity to predict in vivo glioma growth. *J. R. Soc. Interface*, 14(128), 2017.

[40] D. A. Hormuth, A. G. Sorace, J. Virostko, R. G. Abramson, Z. M. Bhujwalla, P. Enriquez-Navas, R. Gillies, J. D. Hazle, R. P. Mason, C. C. Quarles, J. A. Weis, J. G. Whisenant, J. Xu, and T. E. Yankeelov. Translating preclinical MRI methods to clinical oncology. *J. Magn. Reson. Imaging*, 50(5):1377–1392, 2019.

[41] V. S. Goldmacher and Y. V. Kovtun. Antibody-drug conjugates: using monoclonal antibodies for delivery of cytotoxic payloads to cancer cells. *Ther. Deliv.*, 2(3):397–416, 2011.